Evaluation of dose reduction and image quality in chest CT using adaptive statistical iterative reconstruction with the same group of patients

L-P QI, PhD, Y LI, MD, L TANG, MD, Y-L LI, MD, X-T LI, MM, Y CUI, PhD, Y-S SUN, MD and X-P ZHANG, MD

Department of Radiology, Peking University School of Oncology, Beijing Cancer Hospital and Institute, Key Laboratory of Carcinogenesis and Translational Research (Ministry of Education), Beijing, China

Objectives: The objective of this study was to compare the image quality and radiation dose of chest CT images reconstructed with a blend of adaptive statistical iterative reconstruction (ASIR) and filtered back-projection (FBP) with images generated using conventional FBP.
Methods: Patients with chest CT re-examinations were alternately assigned to two scanners with different reconstruction techniques. The study groups included noise index (NI) 11 with 30% ASIR (A30), NI 13 with 40% ASIR (A40), NI 15 with 50% ASIR (A50) and NI 17 with 60% ASIR (A60), sequentially changed every 2 months. The control images were obtained using FBP and NI 11. All acquisitions were performed with automatic dose modulation. Paired *t*-test and non-parameter test were applied to compare the difference.
Results: The radiation doses were significantly lower in the examinations that used ASIR ($p<0.001$). The mean dose reduction rate was 27.7%, 45.2%, 57.1% and 71.8% for Groups A30, A40, A50 and A60, respectively. The image quality of Groups A30–A50 was not inferior to that of the control examinations. The image noise of Group A60 was greater and subjective image quality was inferior to that of the control.
Conclusions: ASIR enabled the use of a higher NI with automatic dose modulation. With 50% ASIR and a NI of 15, the effective radiation dose was reduced by 57%, without compromising image quality.

Received 24 August 2011
Revised 26 November 2011
Accepted 6 December 2011

DOI: 10.1259/bjr/66327067

The rapid development of imaging techniques has led to a remarkable increase in the use of CT. A 2007 report [1] estimated that more than 68.7 million CT examinations are performed each year in the USA, more than 20 times the number performed in 1980 (3 million). Furthermore, CT is responsible for more than two-thirds of the total radiation dose associated with medical imaging [2, 3]. When a widely publicised article [4] claimed that the estimated cancer risk attributable to CT radiation in the USA had grown from 0.4% to 1.5–2.0% because of the substantial increase in the use of CT, radiation exposure became the focus of increased concern.

Many efforts have been made to investigate effective methods for minimising the radiation dose associated with CT. The adopted approaches include decreasing peak voltage, using low-current (mA) applications and using high pitch, among others [5–8]. Automated tube modulation techniques have produced radiation dose reductions of 40–60% without compromising image quality, and are now routinely used with most scanners [9–10].

Address correspondence to: Professor Xiao-Peng Zhang, Department of Radiology, Peking University School of Oncology, Beijing Cancer Hospital and Institute, Fu Cheng Road 52, Hai Dian District, Beijing 100142, China. E-mail: zxp@bjcancer.org
This work was supported by the National Basic Research Program of China (973 Program) (grant no. 2011CB707705) and National Natural Science Foundation of China (grant no. 30970825).

Adaptive statistical iterative reconstruction (ASIR), another approach for minimising radiation, is a unique CT reconstruction algorithm based on raw pixels compared with the routine use of filtered back-projection (FBP). Theoretically, ASIR is a potential reconstruction algorithm to reduce radiation dose with no effect on image quality [11, 12]. In a study on coronary CT angiography in a large multicentre cohort, ASIR enabled a reduced tube current and a lower radiation dose than FBP, and preserved signal, noise and study interpretability [13]. Preliminary studies of chest and abdomen CT examinations have shown that ASIR images had better image quality and less image noise at a lower radiation dose than images acquired with a conventional FBP reconstruction algorithm [14, 15]. In this study, we evaluated the subjective image quality, image noise and radiation dose of chest CT images with automated tube modulation techniques reconstructed with a blend of ASIR and FBP compared with conventional FBP for the same patient group.

Methods and materials

Authors with no financial ties to GE Healthcare had complete, unrestricted access to the study data and unrestricted control over the data during the study. Our prospective clinical study was approved by the human research committee of our institutional review board.

Subjects and methods

The local institutional review board approved this study with a waiver of informed consent. The participants were all adult patients with solid tumours who underwent restaging, evaluation of treatment effect or routine follow-up re-examinations with chest CT scans between 1 September 2010 and 9 April 2011.

The clerical booking team alternately scheduled patients to one of two 64-MDCT scanners. One scanner (Discovery® HD 750; GE Healthcare, Waukesha, WI) was equipped with both ASIR and FBP image reconstruction algorithms. This scanner was capable of generating images with a mix of ASIR and FBP reconstruction algorithms varying from 10% to 100% ASIR in 10% increments. The researcher prospectively designed the reconstruction parameters, including ASIR and noise index (NI; quantum noise level in the image data regulated and desired by the user). We adopted NI 11 with 30% ASIR (A30; based on recommendations from the vendor and the results of initial image quality assessments), NI 13 with 40% ASIR (A40), NI 15 with 50% ASIR (A50) and NI 17 with 60% ASIR (A60). The reconstruction parameters sequentially changed every 2 months, while the other parameters remained constant. For the first few days that the new parameters were adopted, two experienced radiologists reviewed the CT images to ensure their quality. When the quality of the images significantly decreased, the study was stopped. On the fourth day after A60 was adopted, we stopped the study.

The other CT scanner (LightSpeed® VCT; GE Healthcare) was equipped with only a conventional FBP reconstruction algorithm and NI 11 was used as the control.

CT data acquisition

The scanning range of the two scanners went from the supraclavicular space to the upper abdomen, including the bilateral adrenals.

The image acquisition parameters were as follows: tube potential, 120 kV; variable tube current (10–300 mA for the Discovery HD 750 and 50–400 mA for the LightSpeed VCT) determined by *x*-, *y*- and *z*-axis dose modulation; pitch, 0.984:1; table speed, 39.37 mm per gantry rotation; detector configuration, 64×0.625 mm; reconstructed slice thickness, 5 mm; reconstructed interval, 5 mm; gantry rotation time, 0.8 s; field of view appropriate to patient size; and standard (mediastinal) and bone (lung) reconstruction kernels.

For contrast-enhanced CT, a mechanical injector (Stellant®; Medrad, Warrendale, PA) was used for the intravenous bolus injection of non-ionic contrast material (iohexol) with a concentration of 300 mg ml^{-1} iodine. 60–70 ml of contrast material was injected at a flow rate of 2.5 ml s^{-1} and a fixed start delay of 30 s.

Recruiting criteria

The following recruiting criteria were used: (1) the patient had undergone at least one CT examination on each of the two CT scanners; (2) all of the CT examinations of the same patient had either employed contrast medium or had not. If more than one CT examination had the same parameters, then the experimental exam scanned closest to the control one was chosen for the study.

Thoracic CT image analysis

Images obtained with a mediastinal window (window width, 450 HU; window level, 45 HU) and a lung window (window width, 1500 HU; window level, −500 HU) were reviewed at a picture archiving and communication systems (PACS) workstation with all patient and scanner demographic data removed. Two radiologists who had 15 and 10 years of work experience assessed the image quality independently. The readers did not review any previous or subsequent images of any patient, regardless of indication or the presence or absence of a pathological condition. Mediastinal images were assessed with attention to visualisation of the mediastinum, aorta, pulmonary vasculature and chest wall. Lung images were assessed with attention to the bronchial walls and vessels. Image quality problems caused by respiratory motion, patient motion and degree of contrast opacification of the contrast-enhanced images were ignored.

The following three-point Likert scale was used to evaluate image quality [14]. A score of 1 (non-diagnostic) was defined as severely impaired image quality caused by excessive noise, poor delineation of the bronchiolar and/or mediastinal vessel margins, degradation that impeded parenchymal evaluation, and considerable image noise in the chest wall and mediastinal structures. A score of 2 (suboptimal) indicated moderately reduced image quality with limitations in the bronchiolar and/or mediastinal vessel margin delineation, and image noise that limited the evaluation of the pulmonary parenchyma. A score of 3 indicated good image quality without degradation of the bronchiolar and/or mediastinal vessel margin delineation due to image noise and depiction of the pulmonary parenchyma and mediastinal structures that allowed evaluation without substantial noise-related

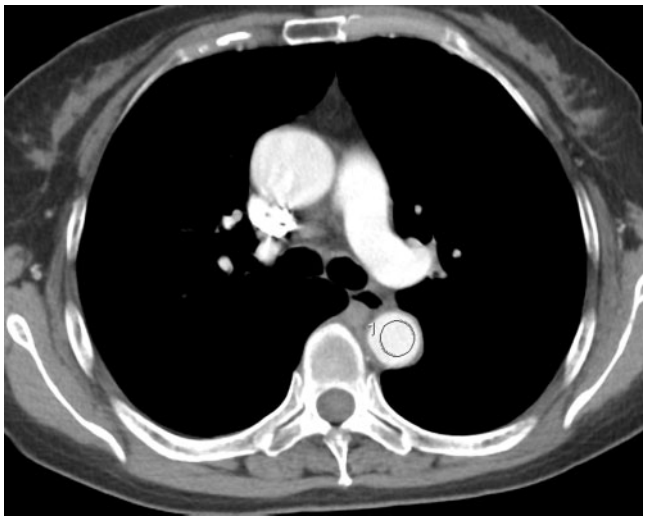

Figure 1. The method of placing a region of interest $>1.0\,cm^2$ in the centre of the descending thoracic aorta at the level of carina in the mediastinal image.

Table 1. Scan ranges of chest CT scans

Group	Control (mm)	With ASIR (mm)	*t*	*p*-value
A30	307±22	306±20	0.391	0.699
A40	311±21	316±22	−1.675	0.105
A50	301±25	304±28	−1.019	0.315
A60	306±22	312±23	−2.365	0.029[a]

A30, noise index 11 with 30% ASIR; A40, noise index 13 with 40% ASIR; A50, noise index 15 with 50% ASIR; A60, noise index 17 with 60% ASIR; ASIR, adaptive statistical iterative reconstruction.
[a]Significant value.

degradation. The recorded image quality score for the examination was the lowest score after review of all mediastinal and lung images.

We measured the noise of the PACS images by placing an oval or circular region of interest $>1.0\,cm^2$ in the centre of the descending thoracic aorta at the level of carina in the mediastinal images (Figure 1). The mean CT value and the standard deviation (SD) from the region of interest were recorded. The mean value for this homogeneous soft tissue was interpreted as the signal, and the SD was interpreted as the noise.

According to department protocol, a screen capture of the scanner console protocol page was sent to the PACS system. This protocol page was reviewed in a separate reading session to record the scan length, the volume CT dose index ($CTDI_{vol}$) and the dose–length product for each CT acquisition. We converted the dose–length product to an effective dose in millisieverts by multiplying it by the thoracic conversion factor of $0.017\,mSv\,mGy^{-1}\,cm^{-1}$ [16].

Statistical analysis

The paired Student's *t*-test (SPSS® for Windows, v. 11.5; SPSS, Inc., Chicago, IL) was used to compare the range of the CT scans and the effective doses between groups. A non-parametric test of two related samples (the Wilcoxon signed-rank test) was applied to compare the image signal-to-noise ratio (SNR), noise and image quality grades. $p<0.05$ was considered statistically significant.

Results

81 patients (42 females and 39 males; age range 20–82 years; mean 56 years) with a total of 199 examinations were recruited into this study. Each patient had 2–4 examinations (48 participants had 2 examinations, 29 had 3 and 4 had 4). All of the patients had control examinations with FBP reconstruction. The number of cases in Groups A30, A40, A50 and A60 was 34, 30, 34 and 20, respectively. 67 patients underwent contrast-enhanced CT examinations, and 14 received plain scans.

Radiation dose

The mean scan lengths for each group and their corresponding control examinations are listed in Table 1. The mean scan length for A60 was longer than that for the control examinations. There were no differences between the other groups and their corresponding controls. The mean radiation doses of the study groups with ASIR were all significantly lower than those of the control groups (paired *t*-test; $p<0.001$ for all). The mean effective doses (ED) for the controls and the study groups were 8.7 *vs* 6.3 for A30, 8.5 *vs* 4.7 for A40, 7.9 *vs* 3.4 for A50 and 9.5 *vs* 2.6 mSv for A60. The mean ED reduction rates for A30, A40, A50 and A60 were 27.7%, 45.2%, 57.1% and 71.8%, respectively (Table 2). The mean dose value of $CTDI_{vol}$ for each group and the corresponding control group are shown in Table 3.

Image characteristics

The SNR and noise values of the CT examinations employed contrast medium are listed in Table 4. The mean SNR of the images of Groups A30, A40 and A50 was not different from that of the control group. The mean SNR of A60 was lower than that of the control group with a marginal significance ($p=0.07$). The image noise of A60 was greater than that of the control group ($p=0.001$).There were no significant differences between A30/A40/A50 and the control group (Figure 2).

Image scores

Detailed scores of two readers are shown in Table 5. The κ-value is 0.214 ($p=0.001$) with agreement in 88.9% (177/199) of cases. There were no cases scored as 1 by either reader. All of the images in the control group were scored as 3 by both observers. Detailed scores of Reader 2 are shown in Table 6. The study group of A50 and A60 showed significantly lower scores than their controls ($p=0.014$, $p=0.005$).

Discussion

Strategies for CT radiation dose optimisation include tube current modulation, body mass index-based tube

Table 2. Radiation dose distribution between control and study group with different percentage ASIR

Group	*n*	Control (mSv)	With ASIR (mSv)	Reduction rate (%)	*t*	*p*-value
A30	34	8.7±3.7	6.3±3.0	27.7±16.5	8.182	<0.001[a]
A40	30	8.5±3.0	4.7±2.2	45.2±14.6	10.722	<0.001[a]
A50	34	7.9±3.7	3.4±2.1	57.1±9.5	12.213	<0.001[a]
A60	20	9.5±2.8	2.6±0.6	71.8±5.4	12.941	<0.001[a]

A30, noise index 11 with 30% ASIR; A40, noise index 13 with 40% ASIR; A50, noise index 15 with 50% ASIR; A60, noise index 17 with 60% ASIR; ASIR, adaptive statistical iterative reconstruction; *n*, number of cases.
[a]Significant value.

Table 3. $CTDI_{vol}$ between control and study group with different percentage ASIR

Group	*n*	Control (mGy)	With ASIR (mGy)	Reduction rate (%)	*t*	*p*-value
A30	34	14.5±6.2	10.6±5.0	28.2±15.6	7.334	<0.001[a]
A40	30	14.0±4.9	7.6±3.7	46.0±14.4	11.309	<0.001[a]
A50	34	13.4±6.4	5.7±3.7	57.3±10.1	11.875	<0.001[a]
A60	20	15.9±5.1	4.3±1.1	72.4±5.3	12.128	<0.001[a]

A30, noise index 11 with 30% ASIR; A40, noise index 13 with 40% ASIR; A50, noise index 15 with 50% ASIR; A60, noise index 17 with 60% ASIR; ASIR, adaptive statistical iterative reconstruction; $CTDI_{vol}$, volume CT dose index; *n*, number of cases.
[a]Significant value.

voltage reduction, decreased scan length and low tube current scanning [17]. Automated tube modulation techniques are now routinely used on most scanners to reduce radiation doses [9, 10, 18]. Owing to inherent density differences in the chest, chest imaging with automated tube modulation is advantageous and routinely used in clinical practice.

In recent years, several studies have shown that, in addition to other accepted methods, ASIR is a useful dose reduction tool for chest or abdomen CT [11–15, 19–20]. Theoretically, with ASIR, it is not assumed that noise is evenly distributed across the entire image, unlike with FBP. ASIR consists of two steps. First, the iterative reconstruction algorithm synthesises forward projection for each X-ray projection angle, considering the actual CT scanning process, in which X-ray photons originate from a finite focal spot area and reach detectors after traversing through the object being scanned. Subsequently, the error between this forward projection and the scanner-acquired raw projection data is back-projected to update the image. During this process, statistical information can be incorporated into the measurement, which results in a less noisy image.

NI is one of the important parameters related to image quality with automated tube modulation. With FBP, it is difficult to balance the radiation dose and image quality. If a high NI is adopted, a lower radiation dose will be obtained, but image noise will increase accordingly. The results of this study showed that ASIR allowed the use of a higher NI, which reduced the tube current and radiation dose and allowed the generation of images with significantly reduced noise without compromising image quality.

This study showed the ED of each group with a combination of ASIR and FBP and corresponding increased NI was significantly lower than that of the control group, which had complete FBP reconstruction. The mean ED reduction rate in Group A50 was 57.1%, and the maximum was 77.0%. The mean ED reduction for Group A30 was 27.7% of the conventional FBP reconstruction with the same NI. This result is consistent with the findings of Prakash et al [20], which showed that ASIR was associated with an overall mean decrease of 27.6% in ED. When the ASIR ratio increased from 30% to 50% and the NI correspondingly increased from 11 to 15, the image quality remained stable and diagnostically useful, and the total ED further decreased by approximately 30%. In total, more than a 50% ED reduction was attributable to ASIR. This study confirmed the important role that ASIR plays in ED reduction.

The SNR and noise for Groups A30–A50 showed no difference from the control groups (Figure 2). The noise of Group A30 was lower than that of the control, with the same NI, although no significance was obtained ($p=0.086$). We noted that the noise of A60 was greater than the value of the control group. The SNR of A60 was 10% lower than that of the control group, with $p=0.07$. The subjective score showed that image quality of Groups A50 and A60 was inferior to the corresponding control groups, but for most (82.4%) cases in Group A50 image quality was good, while for 40.0% of cases in Group A60 image quality was suboptimal. Further analysis of images scored as 2 showed impaired image quality manifesting as the obscure delineation of the heart and vessels in the mediastinal window. However, the bronchioles and the depiction of the pulmonary parenchyma or vessel margins in the lung field did not degrade, which may be attributable to the obvious natural contrast between air and vessels (Figure 3).

This study validated ASIR as an effective dose reduction tool, which was also proved by previous studies on the chest [14, 20]. Mitsumori et al [21] have studied the usefulness of automated current modulation for liver imaging. To our knowledge, there were few articles studying the concurrent changes in ASIR and NI using automatic tube current modulation for the chest.

Table 4. SNR and noise of the control group and study groups

		SNR			Noise		
Group	*n*	Control	With ASIR	*p*-value	Control	With ASIR	*p*-value
A30	22	21.6±5.0	22.9±4.2	0.158	10.0±1.5	9.5±1.3	0.086
A40	25	23.5±5.8	23.1±5.7	0.638	9.8±1.8	10.4±2.1	0.199
A50	30	21.3±4.1	20.8±6.7	0.600	10.0±1.7	10.2±1.4	0.761
A60	16	21.0±5.0	18.8±4.9	0.070	10.4±1.4	11.6±1.6	0.001[a]

A30, noise index 11 with 30% ASIR; A40, noise index 13 with 40% ASIR; A50, noise index 15 with 50% ASIR; A60, noise index 17 with 60% ASIR; ASIR, adaptive statistical iterative reconstruction; *n*, number of cases; SNR, signal to noise ratio.
[a]Significant value.

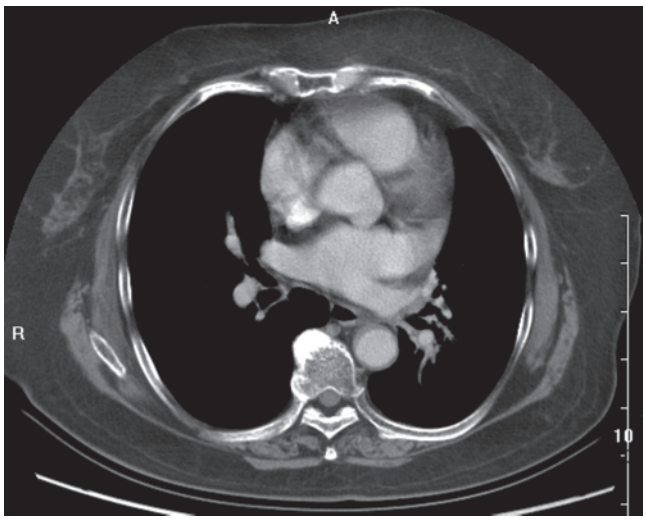

(a)

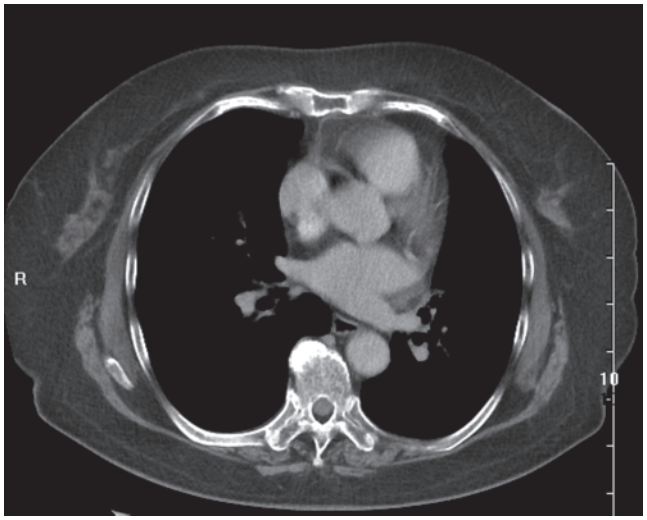

(b)

Figure 2. A 74-year-old female followed up after treatment of left central small cell lung carcinoma. (a) and (b) are images of the same slice obtained under control and A50 conditions in the mediastinal window (width, 450 HU; level, 45 HU). Appearance of aorta and left atrium is similar in (a) and (b), without a difference in image quality despite use of different noise indexes. Both readers assigned Likert score of 3 to both examinations, and measured signal to noise ratio was 19.18 and 13.60 for (a) and (b) conditions, respectively. The calculated effective radiation doses of (a) and (b) conditions were 12.99 and 4.79 mSv, respectively.

Table 5. Detailed scores of two readers

		Reader 2			
	Score	1	2	3	Total
Reader 1	1	0	0	0	0
	2	0	4	6	10
	3	0	16	173	189
Total		0	20	179	199

Table 6. Scores of all the CT images of the control and study groups by Reader 2

		Control	With ASIR		
Group	*n*	Score 3	Score 2 (%)	Score 3 (%)	*p*-value
A30	34	34	3 (8.8)	31 (91.2)	0.083
A40	30	30	3 (10.0)	27 (90.0)	0.083
A50	34	34	6 (17.6)	28 (82.4)	0.014
A60	20	20	8 (40.0)	12 (60.0)	0.005

A30, noise index 11 with 30% ASIR; A40, noise index 13 with 40% ASIR; A50, noise index 15 with 50% ASIR; A60, noise index 17 with 60% ASIR; ASIR, adaptive statistical iterative reconstruction; *n*, number of cases.

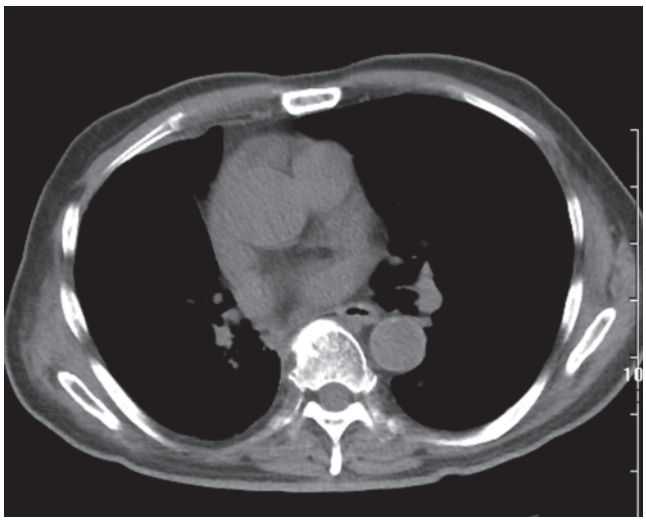

(a)

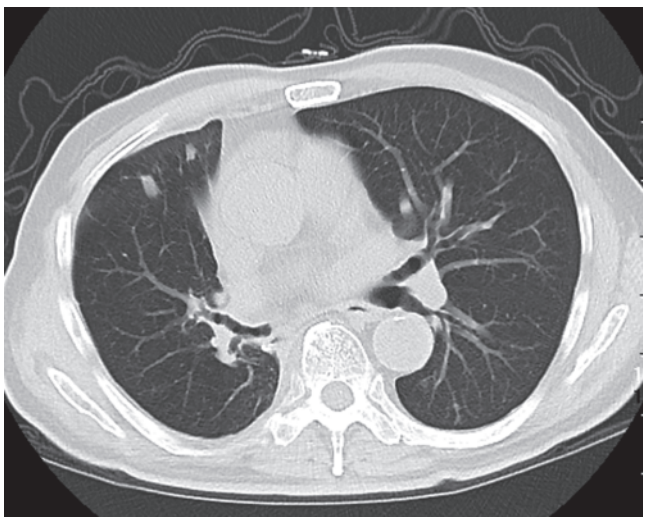

(b)

Figure 3. A 72-year-old male with squamous cell carcinoma received lobectomy of left lower lobe. (a) and (b) are the images under A60 conditions in the mediastinal and lung window. Both readers assigned a Likert score of 2 to the examination. (a) Increased noise and obscure margins in the mediastinal structures. (b) Lung window image, showing clear delineation of the bronchioles and pulmonary vessels.

Our study demonstrated that mean ED acquired with NI 15 and 50% ASIR decreased by 57.1% compared with that obtained with NI 11 and conventional FBP, without obvious decreased image quality. These results provide useful references for ASIR applications with automatic tube current modulation. Because this study was conducted with the same group of patients, patients' weight and body morphology could be ignored, and the results could be used to accurately evaluate the dose reduction of a blend of ASIR and FBP. Another advantage of this study is that it was conducted during clinical practice and did not expose patients to additional radiation.

There are limitations to our study. First, we did not investigate the dose with complete FBP for the Discovery CT750 HD scanner to examine the dose reduction attributable to the hardware and software. Another shortcoming of this work was that we did not investigate the optimal ratio of ASIR to FBP. Nevertheless, our study showed that ASIR allows the use of the higher NI of 15, which was helpful for significantly reducing the radiation dose without impairing image quality. In addition, this study did not consider patient weight change over the course of the study period.

In conclusion, when automatic tube current modulation is adopted, chest CT scans with ASIR allow the use of a higher NI. With an ASIR of 50% and an NI of 15, the effective dose was reduced dramatically, without significantly compromising image quality. This preliminary study validated ASIR as a useful tool to lower radiation doses with a low-dose acquisition mode. Much work remains to be done to optimise the blend of ASIR and FBP and further investigate the maximum noise index.

References

1. IMV Medical Information Division. CT market summary report. Des Plaines, IL: IMV Medical Information Division; 2007.
2. Kalra MK, Maher MM, Toth TL, Hamberg LM, Blake MA, Shepard JA, et al. Strategies for CT radiation dose optimization. Radiology 2004;230:619–28.
3. Linton OW, Mettler FA Jr. National conference on dose reduction in CT, with an emphasis on pediatric patients. AJR Am J Roentgenol 2003;181:321–9.
4. Brenner DJ, Hall EJ. Computed tomography: an increasing source of radiation exposure. N Engl J Med 2007;357: 2277–84.
5. Nakaura T, Awai K, Oda S, Yanaga Y, Namimoto T, Harada K, et al. A low-kilovolt (peak) high-tube current technique improves venous enhancement and reduces the radiation dose at indirect multidetector-row CT venography: initial experience. J Comput Assist Tomogr 2011;35:141–7.
6. Schueller-Weidekamm C, Schaefer-Prokop CM, Weber M, Herold CJ, Prokop M. CT angiography of pulmonary arteries to detect pulmonary embolism: improvement of vascular enhancement with low kilovoltage settings. Radiology 2006;241:899–907.
7. O'Connor OJ, Vandeleur M, McGarrigle AM, Moore N, McWilliams SR, McSweeney SE, et al. Development of low-dose protocols for thin-section CT assessment of cystic fibrosis in pediatric patients. Radiology 2010;257:820–9.
8. Lell M, Hinkmann F, Anders K, Deak P, Kalender WA, Uder M, et al. High-pitch electrocardiogram-triggered computed tomography of the chest. Invest Radiol 2009; 44:728–33.
9. Graser A, Wintersperger BJ, Suess C, Reiser MF, Becker CR. Dose reduction and image quality in MDCT colonography using tube current modulation. AJR Am J Roentgenol 2006;187:695–701.
10. Kalra MK, Maher MM, Toth TL, Kamath RS, Halpern EF, Saini S. Radiation from ''extra'' images acquired with abdominal and/or pelvic CT: effect of automatic tube current modulation. Radiology 2004;232:409–14.
11. Yanagawa M, Honda O, Yoshida S, Kikuyama A, Inoue A, Sumikawa H, et al. Adaptive statistical iterative reconstruction technique for pulmonary CT: image quality of the cadaveric lung on standard- and reduced-dose CT. Acad Radiol 2010;17:1259–66.
12. Silva AC, Lawder HJ, Hara A, Kujak J, Pavlicek W. Innovations in CT dose reduction strategy: application of the adaptive statistical iterative reconstruction algorithm. AJR Am J Roentgenol 2010;194:191–9.
13. Leipsic J, Labounty TM, Heilbron B, Min JK, Mancini GB, Lin FY, et al. Estimated radiation dose reduction using adaptive statistical iterative reconstruction in coronary CT angiography: the ERASIR study. AJR Am J Roentgenol 2010;195:655–60.
14. Leipsic J, Nguyen G, Brown J, Sin D, Mayo JR. A prospective evaluation of dose reduction and image qualitY in chest CT using adaptive statistical iterative reconstruction. AJR Am J Roentgenol 2010;195:1095–9.
15. Sagara Y, Hara AK, Pavlicek W, Silva AC, Paden RG, Wu Q. Abdominal CT: comparison of low-dose CT with adaptive statistical iterative reconstruction and routine-dose CT with filtered back projection in 53 patients. AJR Am J Roentgenol 2010;195:713–9.
16. Bongartz G, Golding SJ, Jurik AG, Leonardi M, van Persijn van Meerten E, Rodriguez R, et al. European guidelines for multislice computed tomography: appendix C. Contract no. FIGM-C T2000-20078-CT-TIP. Luxembourg, Luxembourg: European Commission; 2004.
17. Kubo T, Lin PJ, Stiller W, Takahashi M, Kauczor HU, Ohno Y, et al. Radiation dose reduction in chest CT: a review. AJR Am J Roentgenol 2008;190:335–43.
18. McCollough CH, Bruesewitz MR, Kofler JM Jr. CT dose reduction and dose management tools: overview of available options. Radiographics 2006;26:503–12.
19. Singh S, Kalra MK, Gilman MD, Hsieh J, Pien HH, Digumarthy SR, et al. Adaptive statistical iterative reconstruction technique for radiation dose reduction in chest CT: a pilot study. Radiology 2011;259:565–73.
20. Prakash P, Kalra MK, Digumarthy SR, Hsieh J, Pien H, Singh S, et al. Radiation dose reduction with chest computed tomography using adaptive statistical iterative reconstruction technique: initial experience. J Comput Assist Tomogr 2010;34:40–5.
21. Mitsumori LM, Shuman WP, Busey JM, Kolokythas O, Koprowicz KM. Adaptive statistical iterative reconstruction versus filtered back projection in the same patient: 64 channel liver CT image quality and patient radiation dose. Eur Radiol 2012;22:138–43.